MONITORING OF MAGNETOTELLURIC FIELDS IN THE CENTRAL REGION OF VANCOUVER ISLAND BRITISH COLUMBIA, CANADA

An Internal Report 85-1

D.R. Auld

T.C. Bunyan*

L.K. Law

* Deceased July 2, 1984

T.C. BUNYAN

It is with great sadness we report the death of Thomas C. Bunyan on July 2, 1984.

Mr. Bunyan began his work with the Department at Meanook Magnetic Observatory in 1957. He transferred to the Pacific Geoscience Centre in Sidney, B.C. in 1976. Mr. Bunyan was officer-in-charge of the Victoria Magnetic Observatory from this time until his untimely death this year. He also made a valuable contribution to the seismic program of the Geoscience Centre, to the British Columbia repeat station network, and to the many field projects carried out by the geomagnetic section.
Mr. Bunyan was a close colleague and friend; he will be sadly missed.

ABSTRACT

Beginning in the fall of 1980, a series of magnetotelluric measurements have been made in the central region of Vancouver Island. The purpose of the experiment is to determine if electromagnetic parameters, such as geomagnetic transfer functions or impedance tensor elements, are suitable as precursors to earthquake occurrence.

Seven data sets have been obtained to date: fall 1980; spring and fall 1981 and 1982; and spring, 1983 and 1984. The data have been analysed using transfer function and impedance tensor techniques.

The error bars associated with the electromagnetic parameters derived from data measured at the two sampling rates, 2 second and 20 second, are discussed. One of the impedance tensor elements derived from 20 second data, I_{yx}, is determined to be best suited for monitoring temporal impedance change in the region. Plots of percentage change with time in this I_{yx} element indicate there has been no significant change over the three year period of the experiment.

In addition to the standard MT measurements noted above, in June of 1984, a data set was obtained at one of the sites using the Phoenix Geophysics system. These measurements have established an initial baseline value, in the higher frequency ranges, in order to monitor impedance changes in future years.

INTRODUCTION

In the past two decades there have been dramatic advances in the field of earthquake prediction. During this period, earthquake prediction has reached a stage of scientific credibility. Geophysicists now believe that earthquakes may be preceded by anomalous changes in such phenomenae as tilt, strain, seismic velocities, magnetic field and electrical resistivity. These precursor signals may precede the onset of an earthquake by a matter of hours, days or years. Many countries, notably China, Japan, U.S.A., and U.S.S.R., now have extensive programs to monitor such possible precursors to earthquake occurrence.

The dilatancy model of the earth's crust provides a physical model to explain how these precursor signals may occur prior to a seismic event. Dilatancy is an inelastic volume increase in stressed rock which occurs prior to fracture. The volume increase is produced by new pores and microcracks forming and propagating within the rock due to the steady increase in tectonic stress. Thus the dilatancy model predicts a decrease in electrical resistivity in the focal region of a forthcomng earthquake as a result of water diffusion into the newly created microcracks. Therefore, it may be possible to detect a change with time in impedance at suitably located sites.

The prediction of Feb. 5, 1975 earthquake of magnitude 7.3, which occurred near the town of Haicheng, Liaoning Province, China, is the most important, and accurate, prediction to date. It saved many thousands of lives and many more tens of thousands from serious injury. The prediction, made less than a day before the earthquake, can be considered as a textbook example of the types of precursors that may occur prior to

a large earthquake. Precusor effects were observed in foreshocks, water well levels, radon concentrations, tilt data, geomagnetic data, telluric currents and animal behaviour.

Yamazaki (1977) concludes that, in Japan, measurement of resistivity rather than earth currents is more successful as a precursor monitor. Using a resistivity variometer which he developed, he observed anomalous variations in the rate of change in apparent resistivity preceding a number of Japanese earthquakes. In the seismically active area of the Pamirs, U.S.S.R., Barsukov (1972) made measurements of the electrical resistivity of rocks by means of the dipole-dipole artificial source method. His results show all strong earthquakes measured at stations less than 10 km from his recording site were preceded by a decrease in resistivity. The amplitude of the decrease was 15 to 18% and the duration of the order of a few months.

Canadian earthquake prediction studies using the magnetotelluric method to determine impedance began in 1974 in the province of Quebec. The area chosen for the study, Charlevoix County, is near a centre of seismicity on the north shore of the St. Lawrence River. Data from a number of MT stations established in the region were analysed by Kurtz and Niblett, 1978. Their results showed large changes in the impedance tensor, approximately a 14% increase per year; however, they did not find any clear association between seismic activity and resistivity change. Data are continuing to be measured in this ongoing project.

Kurtz and Niblett, 1983, set up three MT sites north of Baie Comeau, Quebec in response to a series of small earthquakes that were associated with the filling of the Manic 3 reservoir in 1975. The sites were operated for 1 1/2 years but the seismic activity, after the sites were

set up, decreased to very low levels and no significant changes in the EM parameters were measured.

Western Canada has areas affected by the highest seismicity in Canada. This includes the central region of Vancouver Island where numerous large earthquakes have occurred during the last 100 years. Its seismic history makes it a most suitable region to conduct an experiement in the measurement of earthquake precusor phenomena.

Beginning in the fall of 1980, we have made a series of magneto-telluric measurements in the central region of Vancouver Island. The purpose of the experiment is to determine if electromagnetic parameters, such as geomagnetic transfer functions or impedance tensor elements, are suitable for monitoring possible earthquake precursors in this area.

Seven data sets have been obtained to date, fall 1980; spring, fall 1981 and 1982; and spring 1983 and 1984. During the first part of the experiment, our efforts were concentrated on obtaining data at a 2 second sampling interval. For the last two data sets, the emphasis was placed on measuring data at a 20 second sampling interval. The data have been analysed using transfer fraction and impedance tensor techniques and the results are presented in this report.

In addition to the standard MT measuements above, in June of 1984, a data set was obtained at one of the sites using the Phoenix Geophysics system. Results for this data set are also included.

TECTONIC SETTING

The tectonic setting of the central Vancouver Island region is complex. The plate boundaries of the north-east Pacific region are shown in Figure 1. Riddihough (1977) concludes that the two oceanic sub-

plates, Juan de Fuca and Explorer, are interacting independently with the lithosphere beneath Vancovuer Island. He proposes that the present direction of subduction of the Juan de Fuca plate is approximately N 35° E to N 50° E with a convergence rate of 3.5 cm/year; whereas the direction of subduction for the Explorer plate is approxiamtely N 6° E with a much lower rate of subduction. Riddihough and Hyndman (1976) conclude that comtempory subduction is occurring under southern Vancouver Island, but the case for active subduction beneath the northern region is not clear.

Hyndman et al., (1979) located a zone of faulting, the Nootka fault zone, in the oceanic lithosphere, which is at least 20 km wide and extends from the northern end of the Juan de Fuca ridge to the continental margin off central Vancouver Island. It is presumed that this fault zone between the two oceanic plates extends beneath Vancouver Island. It is likely that the tectonic forces causing earthquakes on Vancouver Island are a result of some form of stress coupling between the dynamics of the subduction zone and faults in the crust. There are a large number of crustal faults on Vancouver Island, with the dominant fault pattern striking northwest-southeast. One of these northwest trending faults is the Beaufort Range fault which bisects our study area in the central region of Vancouver Island.

EARTHQUAKE HISTORY

The whole western Canada coastal region is seismically active. Figure 2 shows all of the events for the region contained in the Earth Physics Branch Canadian earthquake data file for the period 1900 to 1975 (Milne et al., 1978). Six of these earthquakes, shown in Figure 3, all

having magnitudes greater than 5.0, played a major role in our decision to begin this project. The dates, coordinates, depths and magnitudes of these earthquakes are given in Table 1 (after Rogers, 1979). The June 23, 1946 earthquake of magnitude 7.3, in particular, was an important factor in our choice of location of sites. Rogers and Hasegawa (1978) studied this earthquake in detail and conclude a preferred location for its epicenter, as shown in Figure 3, is 49.76° N and 125.34° W. In addition, they state that "for one of the northwest striking fault-plane solutions a projection of the fault plane to the Earth's surface coincides with, and is approximately colinear with, a major (Beaufort Range) fault".

STRAIN RELEASE

Figure 4, after Milne et al., 1978, shows plots of strain release as a function of time for two different areas. The two areas, termed Offshore and Continental, are defined by the open dashes in Figure 4. Strain release is calculated as the square root of the total observed seismic energy released during an earthquake.

The character of the strain release is quite different between the two areas. The Offshore area has a relatively smooth slope indicating few large earthquakes, whereas the Continental area has large steps indicating that most of the strain release occurs during large earthquakes. Assuming the rate of strain accumulation is constant with time and that the maximum of the Continental and Offshore curves represent times of minimum accumulated strain, then the dashed straight lines drawn through these maxima, in Figure 4, represent an estimate of the strain accumulation rate. Milne et al., 1978 state, "In the

Continental area it is clear that there is at present, a considerable amount of accumulated strain available for the production of earthquakes. If the historical seismicity pattern continues, a major part of this strain accumulation may be expected to be released in a significant earthquake sometime in the next decade". Since 1975, which is the extent of the plots shown in Figure 4, there have been no large earthquakes in the Continental region and thus the continuation to the present of the strain release curve is essentially flat (horizontal). This project was undertaken in an attempt to establish the baseline of a geophysical parameter, namely crustal impedance, before this accumulated strain is released in a major earthquake.

SITE LOCATION

The two sites, Buttle Lake South (BLS) and Wolf Lake (WL), are shown in Figure 5. BLS is approximately 1 km south of the southern end of Buttle Lake and WL is approxiamtely 10 km north west of Courtenay.

Site Coordinates:

BLS	40° 33.5'	125° 32.7'
WL	49° 42.6'	125° 7.1'

Both sites are accessible by logging road. The telluric lines are left year around, and although there has been some breakage due to animals, this has not been a serious problem. The two sites are approximately 35 km apart, although the distance between them by road is in excess of 100 km. As can be seen in Figure 5, the Beaufort Range fault is located between the sites, BLS lying to the west of the fault and WL to the east.

GEOLOGICAL SETTING

The general geology of the mid-Vancouver Island region is illustrated in Figures 6a and 6b (Muller, 1981). The area of the Buttle Lake site lies within the Sicker Group, the oldest stratigraphic unit recognized on Vancouver Island (mid to late Paleozoic), and is subdivided into three formations: Nitinat, Myra and Buttle Lake. Walker et al., (1984) summarize the composition of the three formations as follows. The Nitinat Formation is composed of pyroxene and feldspar porphyritic, basaltic volcanics and volcaniclastics. The Myra Formation conformably overlies the Nitinat Formation and is composed of bedded volcanics, volcaniclastics and sediments. The Buttle Lake Formation, at the top of the Sicker Group in this area, is composed of geoclastic limestone, chert, argillite, minor tuff and greywacke.

FIELD EQUIPMENT

Our Earth Physics Branch (EPB) standard MT system measured variations in 5 components of the natural electomagnetic field. The three components of the geomagnetic variation field were measured using EDA fluxgate magnetometers (Trigg et al., 1971). For temperature stabilization, the detector heads were buried in holes about 1.5 meters in depth. The holes were covered with plywood, plastic and a large mound of soil. The detector heads were set on an aluminuim pipe which was fixed to a 20 kg concrete block. These blocks were left year around, which, combined with the permanently installed telluric lines, made the set up of each reoccupation relatively simple. The potential difference between pairs of electrodes, orientated in the magnetic north-south and magnetic

east-west directions, were measured with the telluric system designed by Trigg (1972). The electrodes were copper-clad iron ground rods 1.8 meters in length. The electrode spacing was 100 meters. The telluric channels were filtered with either a band pass of 1 to 300 seconds for the 2 second sampling rate or a band pass of 10 to 30000 seconds for the 20 second sampling rate. The five channels were passed through an aliasing filter, which had a 3 db point at approximately twice the sampling rate, and recorded digitally on a Datel cassette recorder. The magnetic and telluric systems and the digital recorder were housed in weather-proof aluminuim transit cases. Power was supplied by 12 volt lead-acid batteries.

Numerous problems and difficulties were encoutered in the operation of the standard MT stations; in particular, in obtaining data at the 20 second sampling rate. The time duration between visits to a station is obviously longer for 20 second data compared to 2 second data - 7 days versus 17 hours respectively. The problems included: the digital recorders malfunctioning, failure of magnetometer and telluric amplifier boards, lack of magnetic activity, breakage of telluric lines, theft of batteries and cassettes, and even an attack on the equipment at BLS by, what was quite likely, a bear.

The problem of battery theft at the WL site became a chronic problem during the last two data sessions, spring 1983 and 1984, and we were reluctantly forced to close the station down permanently in April of 1984.

As well as our standard MT systems, the Phoenix geophysics system was also used in the experiment. It measures the same 5 components of the electromagnetic field as the standard system. The two horizontal components of the geomagnetic field are measured by iron core coils 1.78

meters in length and the vertical component by an air coil approximately 6 meters square. The telluric sensors are Pb-PbCl porous pots orientated as above but separated by 40 meters. The sensor processor, located in the middle of the telluric aray, preamplifies all five components and sends them via a 400 meter communication cable to a 16 channel digitizing unit. A 16 bit parallel interface connects the digitizer unit to a HP9845 computer. Power was supplied by a 1500 watt generator. Software is available for on-site calculations of apparent resistivities, impedance phases, tippers, Bostick inversion, coherences and signal to noise ratios.

DATA PROCESSING

The data cassettes from the standard MT systems are transferred to 9 track tape, plotted by computer and edited for errors. The analogue records are then examined and as many 1440 point independent sections of data, termed data samples, as possible are selected. For the 2 second and 20 second sampling rate, 1440 data points represent 48 minutes and 8 hours respectively.

Linear trends were removed by least squares fit and end effects reduced by use of a cosine bell filter at the beginning and end of each 1440 point data sample. Each sample was increased to 2048 points by the addition of zeros. Then, by use of the fast Fourier transform, the samples were transformed into the frequency domain. Spectral and cross-spectral estimates were computed for each sample by band averaging about selected central frequencies by use of a Parazen window. The individual spectral estimates were then averaged to obtain the final spectral values. These were then used to calculate single station

transfer functions and impedance tensor elements. The transfer functions, A and B, were derived from the equation:

$$H_Z = AH_x + BH_y$$

and the impedance tensor elements, I_{xx}, I_{xy}, I_{yx}, I_{yy} were derived from the two equations:

$$E_x = I_{xx} H_x + I_{xy} H_y$$

$$E_y = I_{yx} H_x + I_{yy} H_y$$

where:

H_z is the vertical magnetic component.

H_x, H_y: are the horizontal magnetic components.

E_x, E_y: are the telluric components

x,y: represent the magnetic north-south and magnetic east-west directions respectively.

DISCUSSION

(i) 2-Second Sampled Data

There are typically 5 to 10, 2 second data samples selected from each spring or fall session at BLS and WL. Table 2 shows values of transfer function amplitudes and directions for nine samples of 2 second

data obtained in the fall of 1981 at BLS. The standard deviations shown for this data set are representative of all the 2 second data sets analysed. These standard deviations are very large and preclude any opportunity of determining if the value of the transfer function is changing with time.

From an examination of Figure 7, a typical analogue plot of 2 second data, the reason for the large values of standard deviation is clear. With the existing sensitivity of the magnetometers used, there is not sufficient energy in the magnetic short period band (5 sec to 100 sec.). Thus based on repeated measurements taken when magnetic activity levels were as high as possible, usually K index values of 3-6, parameters derived from data based on the three magnetic components show too high a degree of variability to be useful for the purpose of this experiment.

The energy in the telluric components appears to be quite acceptable for our needs; the difficulty lies with the magnetic components, in particular the vertical magnetic component. It was hoped that a processed value involving only the tellurics and the horizontal magnetic components, such as impedance, would have acceptable standard deviation values.

The impedance tensor elements derived for the same data set as used in Table 2 are shown in Table 3. Although the standard deviations shown are lower than in the transfer function analysis, they are still very high. During the early stages of the project it was hoped that if we were able to record more active sections of data and/or use only the horizontal components of the magnetic field, we would find that certain parameters derived from 2 second data would be useful in this project. However, such is not the case. Using our standard MT system, geophysical parameters computed from data sampled at 2 second intervals have been

shown to have too high a standard error to enable their use as a possible earthquake precusor.

(ii) 20-Second Sampled Data

Data at the 20 second rate were obtained at BLS for all sessions except spring 1982. One session of 20 second data, spring 1983, was obtained at WL. Although WL is now shut down, this data sample is discussed briefly in the following section.

There are six sets of data from BLS. Generally, there is a smaller number of 20 second samples from the first part of the experiment; since, during 1981 and 1982, we concentrated our efforts in obtaining data at the 2 second sampling rate. Figures 8 and 9 show plots of the impedance tensor elements, both real and quadrature, for a good quality data set from BLS, spring 1983. This data set is derived from 10 samples of 8 hours duration each. Figure 8 displays the I_{xy} and I_{xx} impedance tensor elements for a period range from 100 to 3000 seconds. Although the error bars are still large below 300 seconds, they have improved considerably in the period range from 300 to 3000 seconds. In Figure 9, which shows the two impedance elements, I_{yx} and I_{yy}, there is a further reduction in the magnitude of the error bars. Particularly in the real and quadrature components of I_{yx} where the percent error above 300 seconds is about 5 to 15%. A similar result, of lower error bars for the I_{yx} impedance element, was also observed for the other five data sets from BLS. We conclude then that of the electromagnetic parameters we examined, the I_{yx} real and quadrature impedance elements derived from 20 second sampled data are the best parameters to use for this experiment.

Thus in Figure 10 we have selected three periods from each of the 20 second data sets and plotted the change taking place with time in I_{yx}. The vertical axis shows the percentage change in impedance, with the May 1981 value being set to zero. The October 1980 value, although shown, was not selected as the zero value because of a change in electrodes after this data set was obtained. The short galvanized iron electrodes used in the initial set up were replaced in the spring of 1981 by longer, copper-clad iron electrodes. Time is displayed along the horizontal axis, and the three periods plotted are: 135, 335 and 1050 seconds.

Over the duration of the experiment to date, Figure 10 indicates that, within the limit of the error bars, there has been no significant deviation from the zero line for any of the curves displayed. Such a result can be interpreted in several ways. It is possible the region is responding as theory dictates: we are in the early phase of dilatancy - where the accumulation of tectonic strain is producing a steady increase in stress but without an effective increase in porosity. Thus during this phase, the dilatancy model curve of change in impedance with time does indeed remain flat. Other possibilities include: the Buttle Lake site is currently ouside any dilatant region which may exist in the area or the period range used in this study is not responsive to any change in impedance which may be occurring.

Note that, although not statiscally significant, there is a suggestion of a decreasing trend in the real component of I_{yx} for the 1050 second period data. In order to resolve real changes of this magnitude (10 to 15 % over three years) it is necessary to reduce the errors.

(iii) Reduction of Errors

The reduction of errors can be achieved in two ways. First, we need sites which have a low noise level. Figure 11 shows the I_{yx} and I_{yy} impedance elements derived for the May 1983, 20 second data set from Wolf Lake. Although this site is now shut down, the data are being displayed to indicate the small magnitude of the error bar at Wolf Lake. In particular, note the quadrature component above 300 seconds where the error is very low, of the order of a few percent. We've found a possible replacement site for the Wolf Lake station, at an experimental farm operated by University of British Columbia located between Courtenay and Cambell River. It would make a secure site and we are hopeful, if we proceed with it, data would be similar in quality to the Wolf Lake data.

Secondly, we need better instrumentation. In June of 1984, we made measurements at Buttle Lake with the Phoenix Geophysic System. This MT system allows us to establish a good short period reference which we were unable to do from our 2 second data. In fact, the Phoenix system allows measurements to be made down as low as 0.0026 seconds (384 H_z) with the range extending up to 1800 seconds. It is a most impressive system, allowing on site computer processing, with the electromagnetic parameters outputted in the form of numerical tables or plots. Because of the "real time" computations, data collection at each site can be extended until the operator is satisfied that sufficient high quality data have been observed.

We were very pleased with the results of the Phoenix measurements. Figure 12 shows a plot of apparent resistivity and phase versus period for the BLS site obtained directly from the output of the Phoenix system. RHO_{xy} is calculated from E_x/H_y and RHO_{yx} from E_y/H_x. These data are

displayed in table format as well, Table 4, also obtained directly from Phoenix output. Table 4 shows the quality of the data set, the standard deviation values associated with both the apparent resistivity values and phase are extremely low. With such apparent high quality data, we look forward with considerable interest to the next data set obtained at BLS with the Phoenix system. This system, we believe, shows excellent potential for achieving the objective of this experiment: the correlation of change in electrical resistivity with earthquake occurrence.

RECOMMENDATIONS

We are recommending the continuation of the Buttle Lake site and the establishment of one or two new low noise sites in the region. At the sites, measurements would be taken once a year with our standard MT systems. Because of the expense and demands on the Phoenix system, it is unlikely it could be used more than on an every other year basis. Measurements with the Phoenix system, at all sites, would thus be taken whenever possible.

If we detect any change in impedance, or a change in some other geophysical parameter is observed, we would then take observations more frequently. As well, if a large earthquake occurs, with or without a prediction, we would take measurements as soon as possible after its occurrence.

CONCLUSIONS

Geomagnetic transfer functions and impedance tensor elements, computed from data obtained with a standard EPB MT system using a digitizing interval of 2 or 20 seconds, were examined as to their suitablity as earthquake precursor measurements. The parameters derived from the 2 second data obtained with this equipment were shown to have too high a standard error to enable their use for this purpose. In comparison, the error bars associated with impedance tensor elements obtained from the 20 second data were much lower in magnitude. The data showed, in particular, the I_{yx} real and quadrature impedance elements were best suited for monitoring of temporal change in impedance in this region. Baseline curves for a three year period from 1981 to 1984, showing percentage change with time in the I_{yx} element, indicated there has been no statistical deviation from zero during this time.

To date, we have a 100% success rate: we have observed no significant change, we have made no prediction and there has been no large earthquake.

ACKNOWLEDGMENTS

We would like to thank J.M. DeLaurier and R.D. Kurtz for their valuable contribution to the Phoenix Geophysics system field program. We are also indebted to J.M.D. for his useful comments on the manuscript. Our thanks are also extended to G.C. Rogers and H. Dragert for many discussions regardng precursor monitoring in central Vancouver Island.

REFERENCES

Barsukov, O.M., 1972. Variations of electric resistivity of mountain rocks connected with tectonic causes. Tectonophysics, 14, 273-277.

Hyndman, R.D., R.P. Riddihough and R. Herzer, 1979. The Nootka fault zone - a new plate boundary off Western Canada. Geophy. J.R. Astr. Soc., 58, 667-683.

Kurtz, R.D. and E.R. Niblett, 1978. Time dependence of magnetotelluric fields in a tectonically active region in eastern Canada. J. Geomag. Geoelectr., 30, 561-577.

Kurtz, R.D. and E.R. Niblett, 1983. Magnetotelluric monitoring of impedance in an area of induced seismicity at Manic 3, Quebec. Pub. Earth Physics Branch, Ottawa, 25, 1-38.

Milne, W.G., G.C. Rogers, R.P. Riddihough, G.A. McMechan and R.D. Hyndman, 1978. Seismicity of Western Canada. Can. J. Earth Sci., 15, 1170-1193.

Muller, S.E., 1981. Insular and Pacific Belts. Field guides to Geology and mineral deposits, Geological Association of Canada - Mineralogical Association of Canada - Canadian Geophysical Union, Joint Annual Meeting 1981, Calgary, Alberta. 316 - 334.

Raleigh, B., G. Bennett, H. Craig, T. Hanks, P. Molnar, A. Nur, J. Savage, C. Scholz, R. Turner, and F. Wu, 1977. Prediction of the Haicheng Earthquake. EOS, 58, 236-272.

Riddihough, R.P., 1977. A model for recent plate interactions off Canada's west coast. Can. J. Earth Sci., 14, 384-396.

Riddihough, R.P. and R.D. Hyndman, 1976. Canada's active western margin - the case for subduction. Geoscience Canda, 3, 269-278.

Rogers, G.C., 1979. Earthquake fault plane solutions near Vancouver Island. Can. J. Earth Sci., 16, 523-531.

Rogers, G.C. and H.S. Hasegewa, 1978. A second look at the British Columbia earthquake of June 23, 1946. Bull. Seis. Society of America, 68, 653-675.

Trigg, D.F., 1972. An amplifier and filter system for telluric signals. Pub. Earth Physics Branch, Ottawa, 44, 1-5.

Trigg, D.F., P.H. Serson and P.A. Camfield, 1971. A solid state electrical recording magnetometer. Pub. Earth Physics Branch, Ottawa, 41, 67-80.

Walker, R., C. Yorath, A. Sutherland Brown, 1984. Guidebook for second annual fall field trip, "Buttle Lake Mine and Lithoprobe Geology".

Yamazaki, Y., 1977. Tectonoelectricity. Geophys. Surveys, 3, 123-142.

Table 1.

Large magnitude earthquakes occurring in the central Vancouver Island Region

Date	Coordinates	Magnitude
Dec. 6, 1918	49.8 N 126.5 W	7.0
June 23, 1946	49.8 N 125.3 W	7.3
Dec. 16, 1957	49.8 N 126.5 W	6.0
July 5, 1972	49.5 N 127.2 W	5.7
Mar. 31, 1975	49.3 N 126.0 W	5.4
Nov. 30, 1975	49.2 N 123.6 W	4.9

Table 2.

BLS Transfer Function Amplitudes and Directions

PERIOD (sec)	A-REAL	ST.DEV.	A-QUAD	ST.DEV.	B.REAL	ST.DEV.	B-QUAD	ST.DEV.
292	.252	.236	-.038	.182	.121	.074	-.050	.122
215	.228	.182	.019	.216	.160	.107	-.003	.146
163	.266	.284	-.070	.154	.084	.181	-.045	.093
105	.163	.086	-.062	.052	.059	.040	-.027	.063
66	.163	.091	-.039	.104	.054	.081	-.083	.063
41	.004	.112	-.100	.165	.047	.057	-.047	.122
33	.048	.192	-.095	.118	-.040	.182	-.062	.134
26	.134	.219	-.120	.296	.056	.213	-.071	.105
21	.112	.203	.003	.136	.063	.121	.019	.202
16	-.021	.214	.028	.243	.029	.193	-.067	.214
13	.012	.283	.114	.160	-.088	.248	-.015	.230
10	.084	.299	.010	.162	-.029	.278	-.062	.186
8	.151	.282	-.067	.225	-.061	.309	-.015	.314

PERIOD (sec)	MAGN-REAL	ST.DEV.	DIRN.-REAL	ST.DEV.	MAGN-QUAD	ST.DEV.	DIRN.-QUAD.	ST.DEV.
292	.308	.206	25.6	14.1	.141	.174	-127.1	32.0
215	.317	.137	35.1	15.9	.215	.127	-9.9	38.6
163	.317	.296	17.6	15.4	.147	.126	-147.4	22.6
105	.175	.092	19.8	3.1	.089	.053	-156.2	19.9
66	.192	.082	18.3	12.2	.141	.046	-115.3	18.5
41	.121	.045	85.7	24.9	.204	.096	-154.9	27.7
33	.235	.110	-39.7	34.9	.177	.106	-146.8	26.2
26	.291	.146	22.5	21.5	.303	.131	-149.4	26.4
21	.205	.165	29.4	30.2	.203	.115	81.1	35.0
16	.244	.134	125.7	30.8	.300	.097	-67.1	32.6
13	.338	.148	-82.5	28.8	.233	.180	7.2	27.7
10	.332	.227	-18.8	36.9	.226	.088	-81.0	31.2
8	.366	.234	-22.0	31.6	.343	.149	-167.5	30.6

Table 3.

BLS Impedence tensor elements

PERIOD (sec)	I_{xx}-REAL	ST.DEV.	I_{xx}-QUAD	ST.DEV.	I_{xy}-REAL	ST.DEV.	I_{xy}-QUAD	ST.DEV.
292	-.82	1.19	.97	2.34	1.65	1.07	-1.31	.96
215	-.97	1.75	2.67	1.25	.46	1.56	-3.28	1.21
163	-.11	1.59	3.04	2.17	1.32	1.55	-3.81	1.34
105	1.03	.63	3.53	.56	-.59	.60	-5.44	1.08
66	2.77	.57	3.18	1.63	-1.27	1.34	-7.66	1.95
41	3.03	1.85	4.36	1.61	-1.63	1.29	-11.13	2.61
33	3.58	1.39	3.77	2.00	-1.84	1.04	-12.53	4.02
26	3.66	2.97	5.71	3.73	-2.09	1.29	-14.67	4.51
21	3.78	5.16	3.65	5.46	-3.67	2.13	-17.79	6.11
16	-.25	4.82	1.30	3.66	-2.54	3.29	-16.05	8.44
13	-.82	5.26	-1.22	7.23	.73	4.69	-13.71	13.51
10	-.51	6.61	-1.12	7.09	-2.45	4.07	-4.19	4.75
8	1.25	2.59	.33	4.71	.24	4.92	-2.79	4.11

PERIOD (sec)	I_{yx}-REAL	ST.DEV.	I_{yx}-QUAD	ST.DEV.	I_{yy}-REAL	ST.DEV.	I_{yy}-QUAD	ST.DEV.
292	-.86	.63	.77	.58	.33	.18	-.39	.37
215	-.82	.38	1.76	.54	-.01	.54	-.91	.29
163	-.27	.56	2.67	1.03	.31	.42	-.82	.45
105	.46	.35	3.59	.40	-.00	.20	1.16	.35
66	1.51	.43	4.08	.70	.07	.47	-1.79	.48
41	1.77	1.37	4.93	.70	.10	1.02	-2.77	.98
33	2.09	1.12	4.89	1.78	.32	.51	-3.21	1.46
26	2.15	1.53	5.90	1.21	.18	.99	-4.07	1.43
21	1.59	2.36	5.61	4.36	-.12	1.19	-4.83	1.42
16	.90	1.65	4.46	2.57	-.42	2.24	-4.43	1.94
13	.63	2.51	1.98	1.90	1.84	2.75	-3.40	4.12
10	-.75	2.24	1.25	2.04	-.23	1.24	-1.50	1.50
8	-.06	.49	-.06	1.81	-.12	1.40	-1.25	2.21

PHOENIX GEOPHYSICS

MT Site: VANI84-016E

APPARENT RESISTIVITY ESTIMATES

F#	Frq/Prd	STACKS	RHOxy	%SD	RHOyx	%SD	PHASExy	%SD	PHASEyx	%SD
1	384.00 Hz	575	3734.8	8.3	503.3	15.0	3.4	2.3	-139.5	4.0
2	288.00 Hz	725	3631.5	9.3	811.8	8.3	19.9	2.5	-141.1	2.3
3	192.00 Hz	525	1276.8	10.6	263.0	13.6	25.0	2.9	-138.8	3.6
4	144.00 Hz	575	3852.3	2.3	508.1	1.2	28.7	.6	-137.0	.4
5	96.00 Hz	700	4632.1	1.3	531.3	.7	27.8	.4	-141.6	.2
6	72.00 Hz	525	5614.0	1.6	615.1	.9	26.8	.4	-143.6	.3
7	48.00 Hz	750	5999.7	1.5	589.9	1.0	29.5	.4	-144.7	.3
8	36.00 Hz	700	6842.6	1.6	681.7	1.1	30.7	.5	-147.6	.3
9	24.00 Hz	700	7384.5	1.9	749.3	1.3	31.0	.5	-149.5	.4
10	18.00 Hz	700	9089.5	1.8	949.8	1.3	33.6	.5	-149.3	.4
11	12.00 Hz	525	9883.1	1.7	1106.1	1.4	35.7	.5	-149.2	.4
12	9.00 Hz	750	10393	1.0	1161.4	1.0	37.0	.3	-147.2	.3
13	6.00 Hz	750	10776	1.4	1387.7	1.3	41.0	.4	-143.2	.4
14	4.50 Hz	750	11187	1.5	1507.1	1.5	43.1	.4	-139.9	.4
15	3.00 Hz	350	11230	1.5	1497.3	1.4	45.2	.4	-135.0	.4
16	2.25 Hz	573	11384	1.4	1513.7	1.7	48.0	.4	-131.0	.5
17	1.50 Hz	350	10309	2.4	1370.3	2.3	47.6	.7	-128.5	.6
18	1.12 Hz	400	10342	2.4	1335.2	2.3	52.3	.7	-124.1	.6
19	1.33 Sec	3840	9968.5	.9	1101.7	1.0	55.9	.3	-119.9	.3
20	1.78 Sec	4840	8984.0	.9	1045.8	.8	58.1	.3	-118.1	.2
21	2.67 Sec	2060	8270.7	1.0	833.3	1.1	62.1	.3	-114.5	.3
22	3.56 Sec	2395	7646.4	.8	751.4	1.0	64.8	.2	-112.6	.3
23	5.33 Sec	952	6357.9	1.0	581.6	1.8	68.7	.3	-110.5	.5
24	7.11 Sec	952	5273.6	1.3	473.1	2.4	71.2	.4	-110.7	.7
25	10.67 Sec	420	3664.3	1.4	340.2	4.2	71.8	.4	-110.3	1.2
26	14.22 Sec	570	3364.4	1.2	273.1	3.2	68.4	.3	-113.4	.9
27	21.33 Sec	247	2379.2	.9	231.4	2.4	67.1	.2	-113.2	.7
28	28.44 Sec	267	2019.8	.8	208.3	1.8	65.9	.2	-113.3	.5
29	42.67 Sec	167	1779.2	1.1	148.4	4.2	59.7	.3	-111.5	1.2
30	56.89 Sec	260	1557.0	.9	138.9	2.4	56.2	.3	-112.8	.7
31	85.33 Sec	85	1470.4	1.8	126.4	4.1	51.3	.5	-119.0	1.1
32	113.78 Sec	105	1411.4	1.5	127.6	4.4	47.0	.4	-116.7	1.2
33	170.67 Sec	48	1356.6	4.2	124.6	9.1	44.7	1.2	-123.5	2.5
34	227.56 Sec	36	1385.8	2.1	116.5	7.5	42.6	.6	-122.4	2.1
35	341.33 Sec	6	1543.8	4.8	100.1	16.8	40.0	1.3	-129.1	4.4
36	455.11 Sec	30	1494.3	4.6	106.5	10.6	36.1	1.3	-121.9	2.9
37	682.67 Sec	15	1767.5	8.5	56.2	31.7	33.3	2.3	-121.4	7.9
38	910.23 Sec	15	1653.8	5.4	68.7	11.5	32.4	1.5	-111.3	3.1
39	1365.34 Sec	6	2303.6	3.7	63.6	26.4	28.4	1.0	-117.5	6.7
40	1820.46 Sec	6	2111.0	11.8	70.7	22.3	66.9	3.2	-147.4	5.8

Table 4. Apparent Resistivity Estimates for the BLS site obtained directly from the output of the Phoenix Geophysics system.

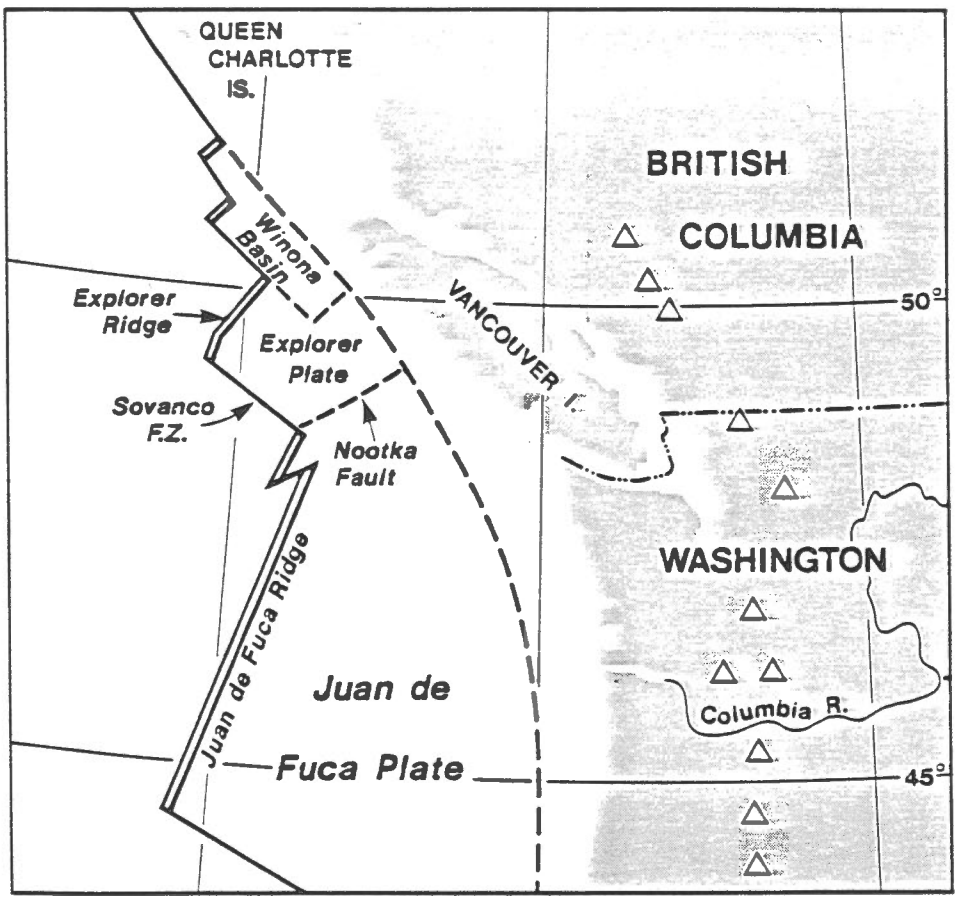

Fig. 1. Tectonic map of western Canada showing the main lithospheric plate boundaries

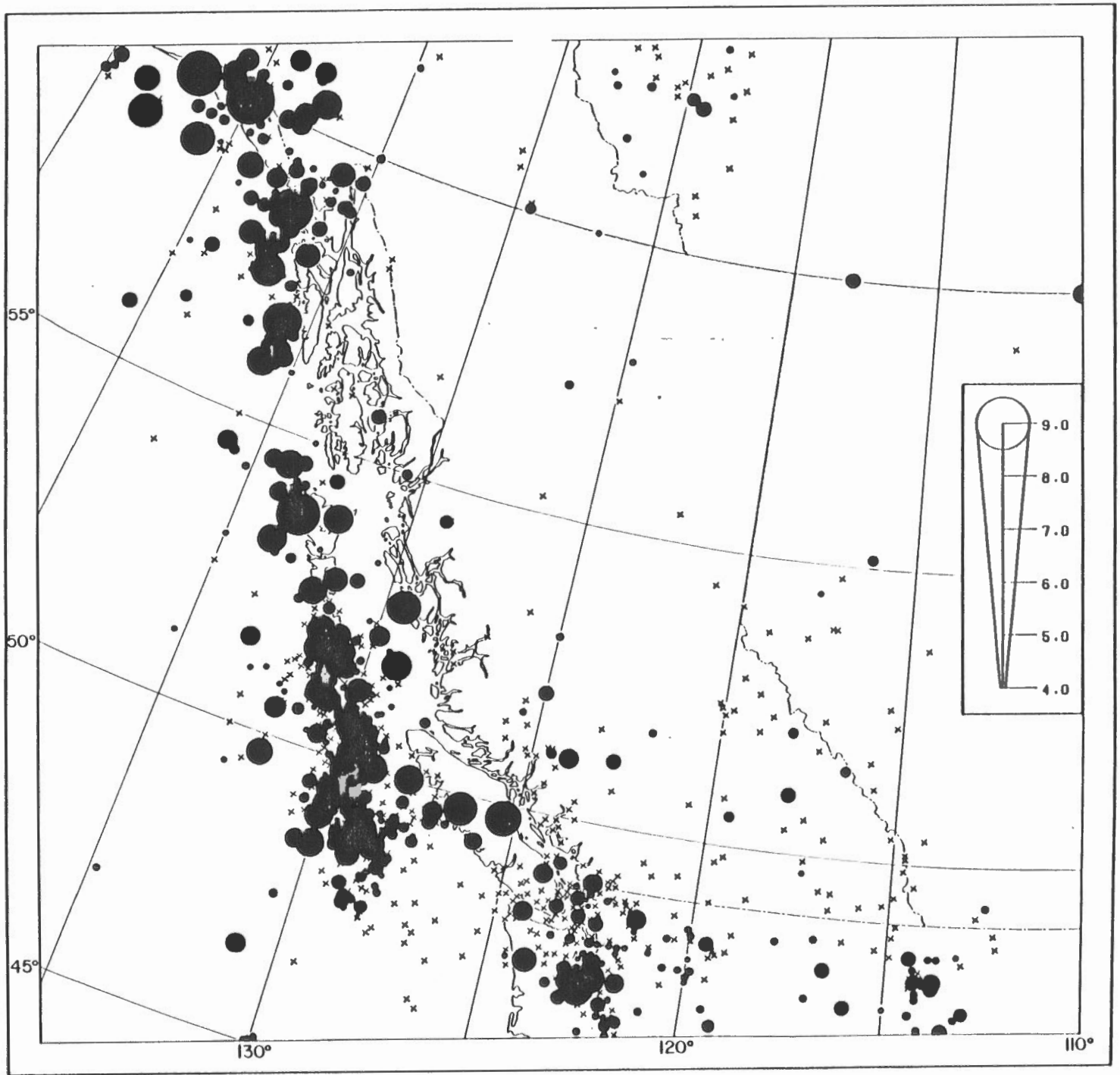

Fig. 2. Western Canada regional distribution of earthquakes with magnitude greater than 3.0 for the period 1899 to 1975. Earthquakes of magnitude less than 4.0 are marked by "X".

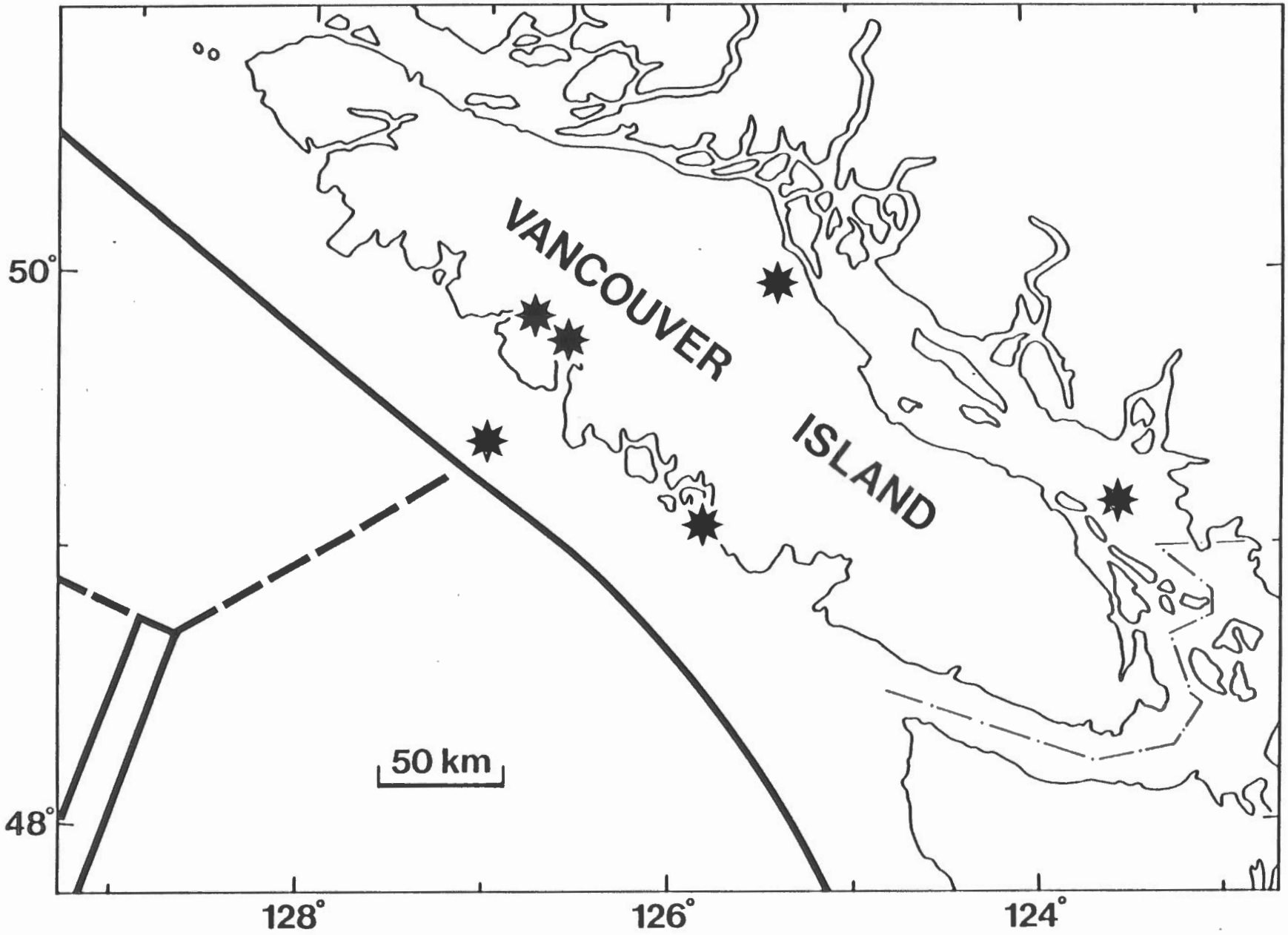

Fig. 3. Location of six major earthquakes which have occurred near the study area

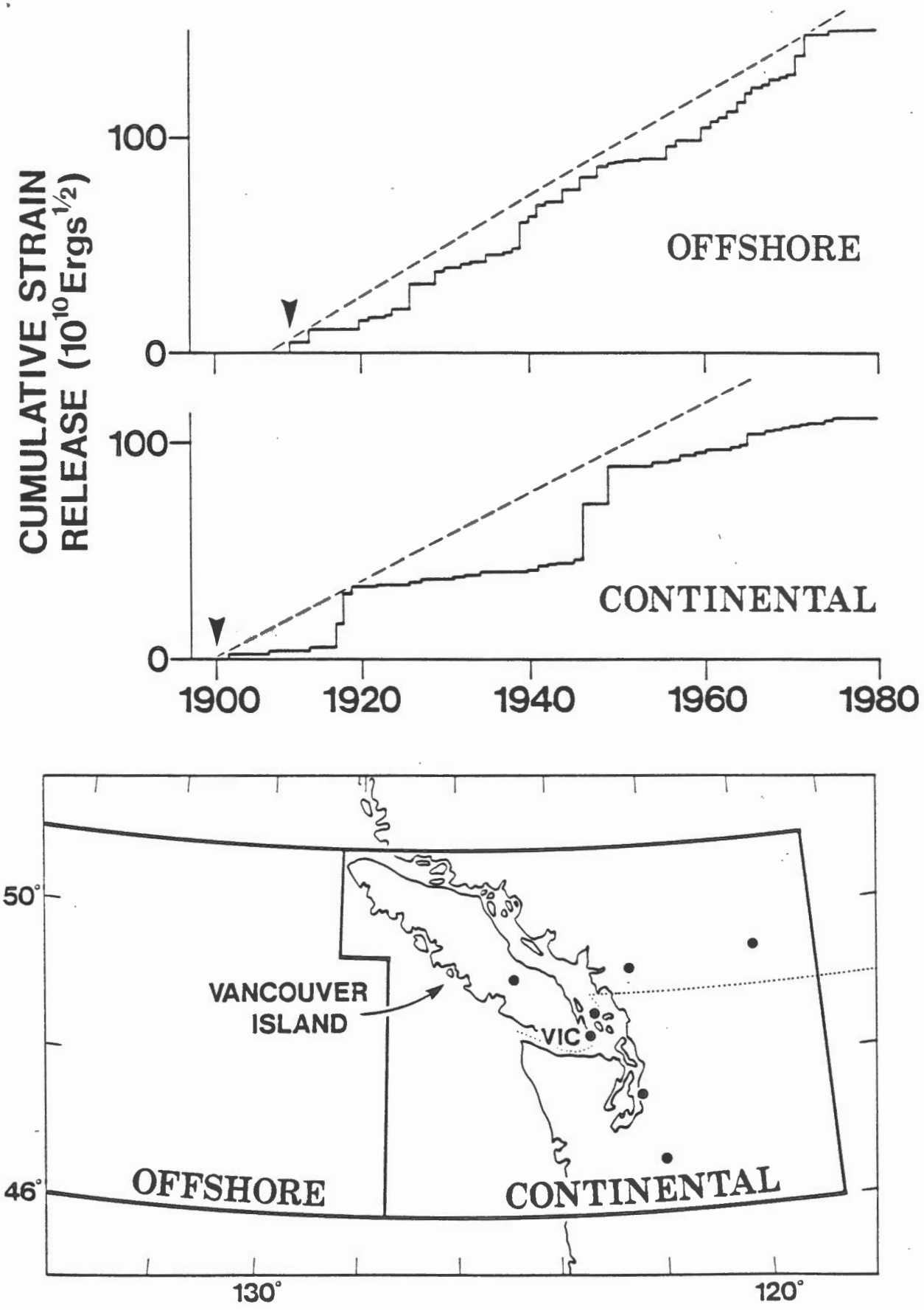

Fig. 4. Strain release as a function of time for the offshore and continental regions

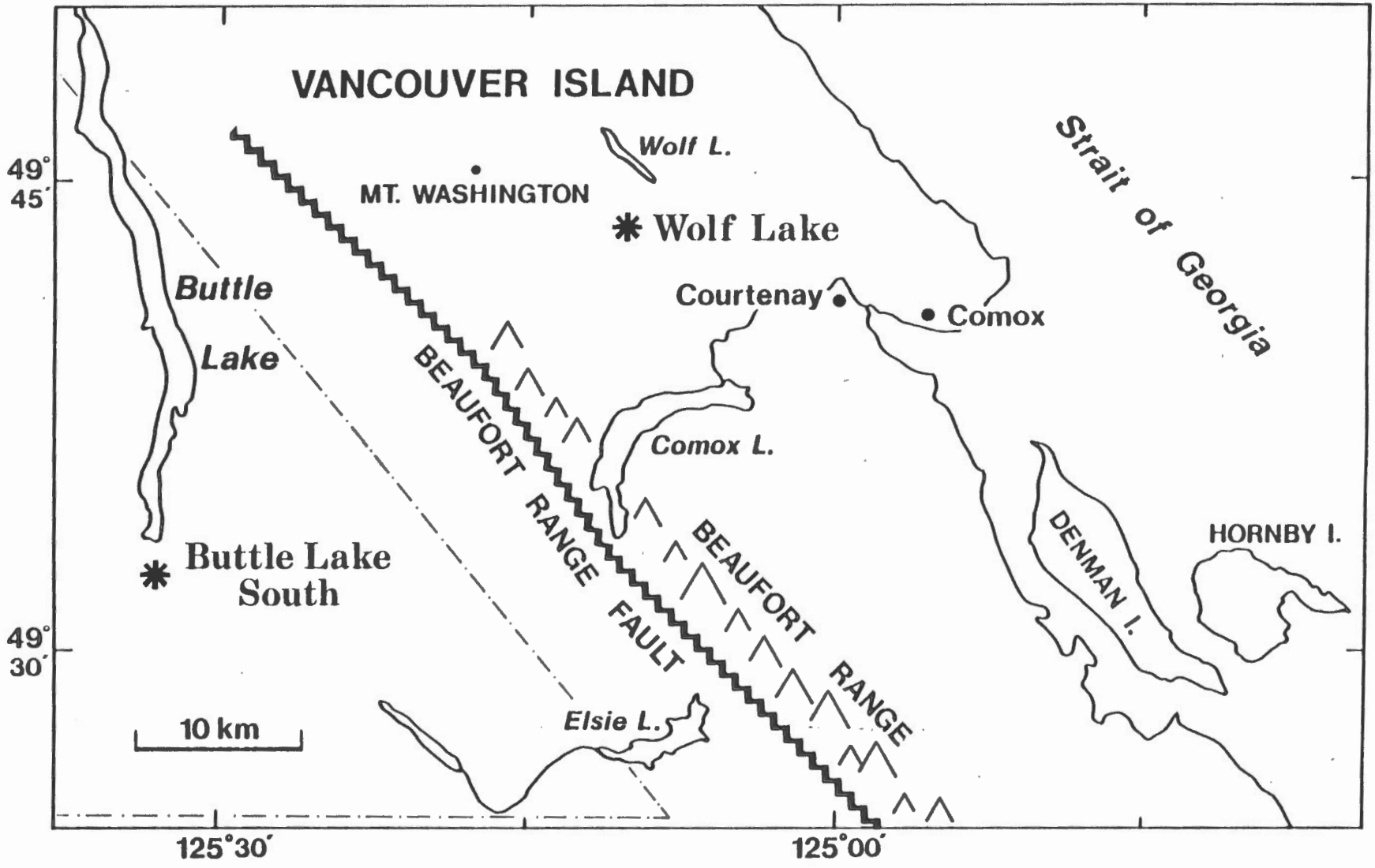

Fig. 5. Location of magnetotelluric recording sites at Buttle Lake South and Wolf Lake and the Beaufort Range Fault

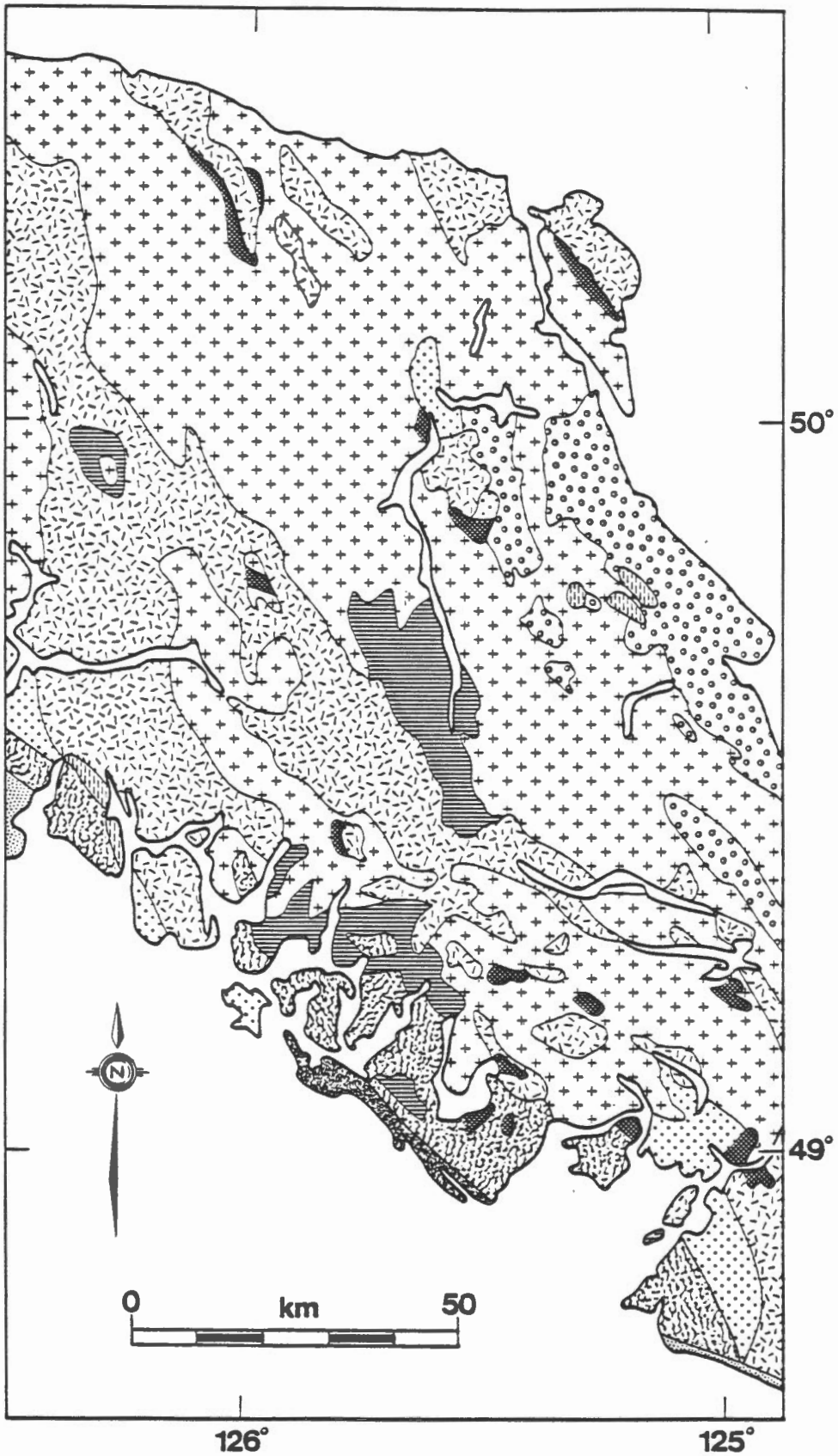

Fig. 6(a). General geology of the central Vancouver Island region (after Muller, 1981)

Fig. 6(b). General geology of the central Vancouver Island region (after Muller, 1981)

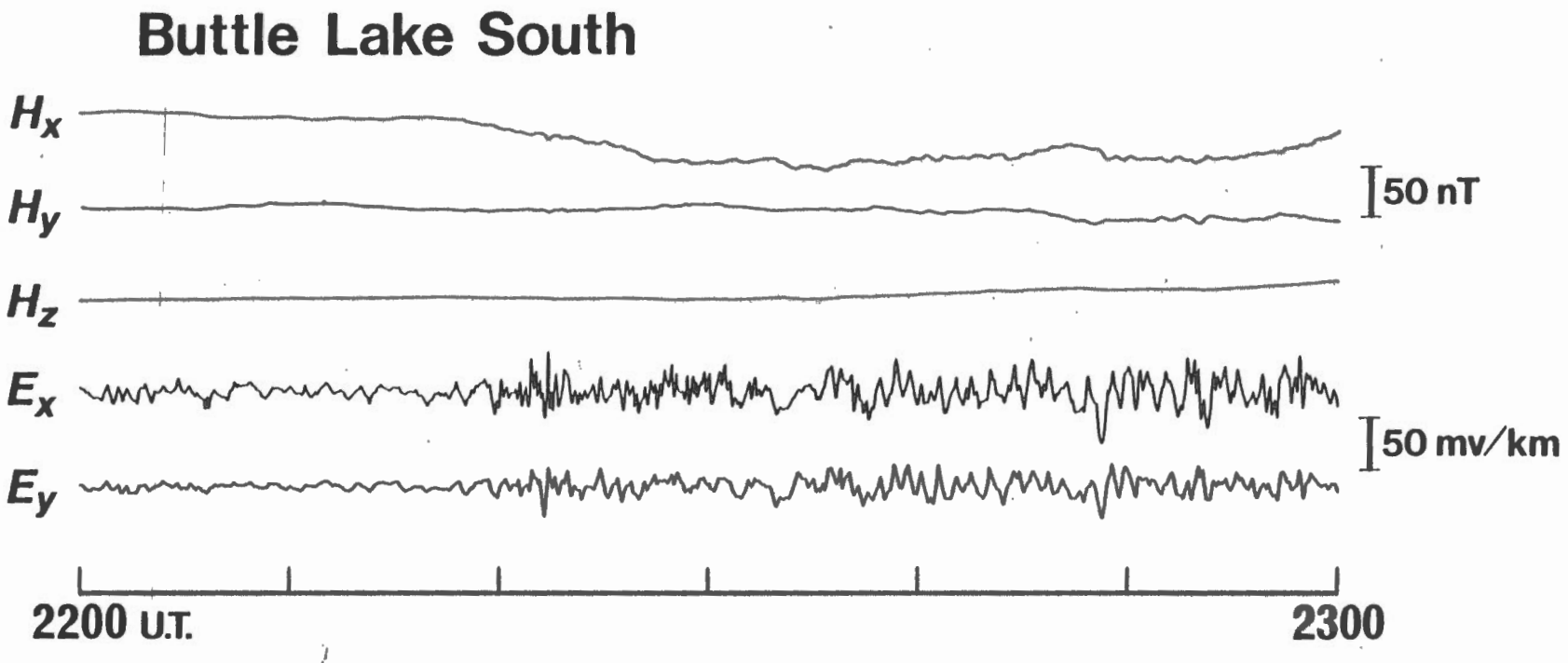

Fig. 7. Plot of two second data from BLS: 2200 to 2300 May 27, 1982 UT.

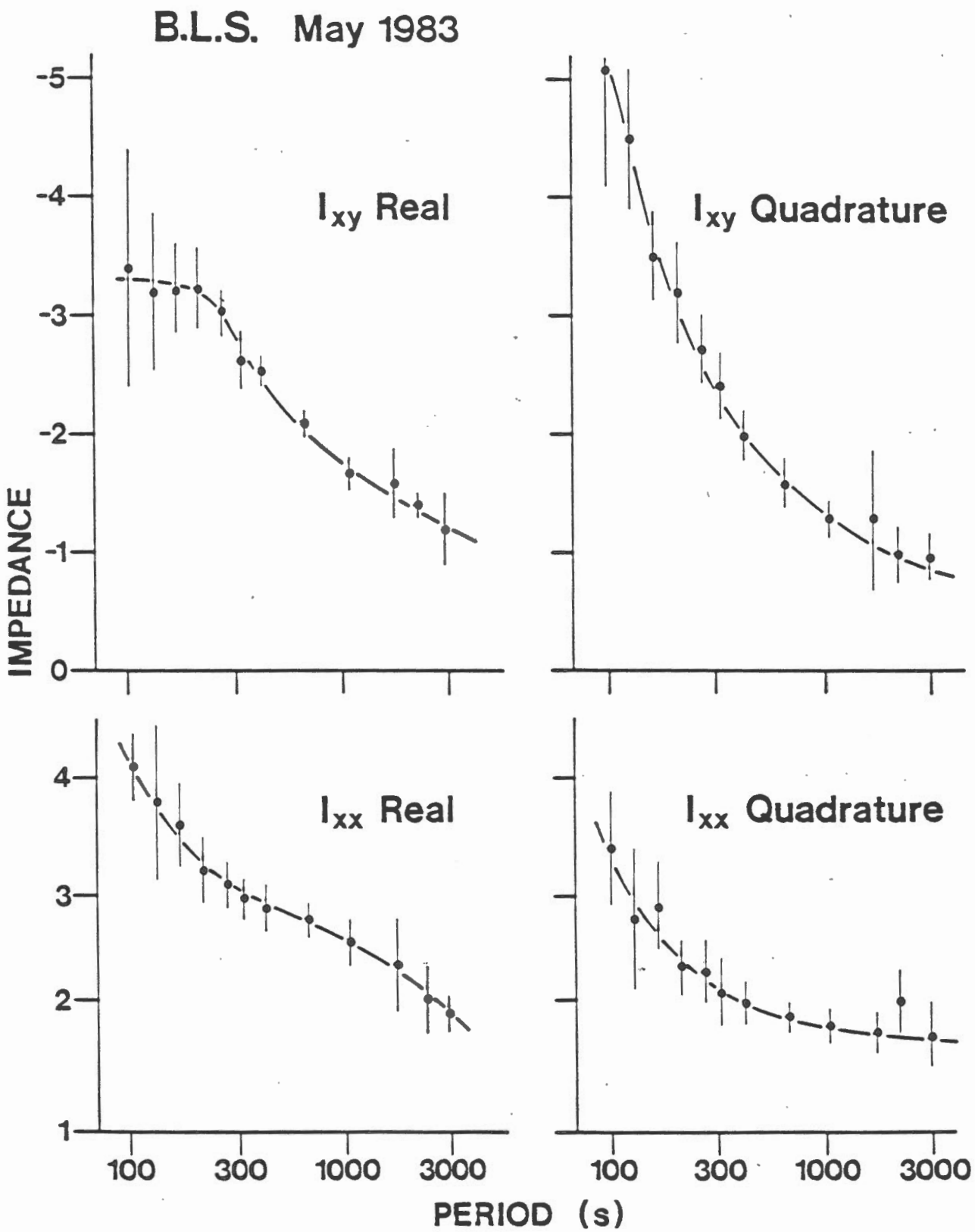

Fig. 8. I_{xy} and I_{xx} Impedance tensor elements, real and quadrature, derived from twenty second data from BLS

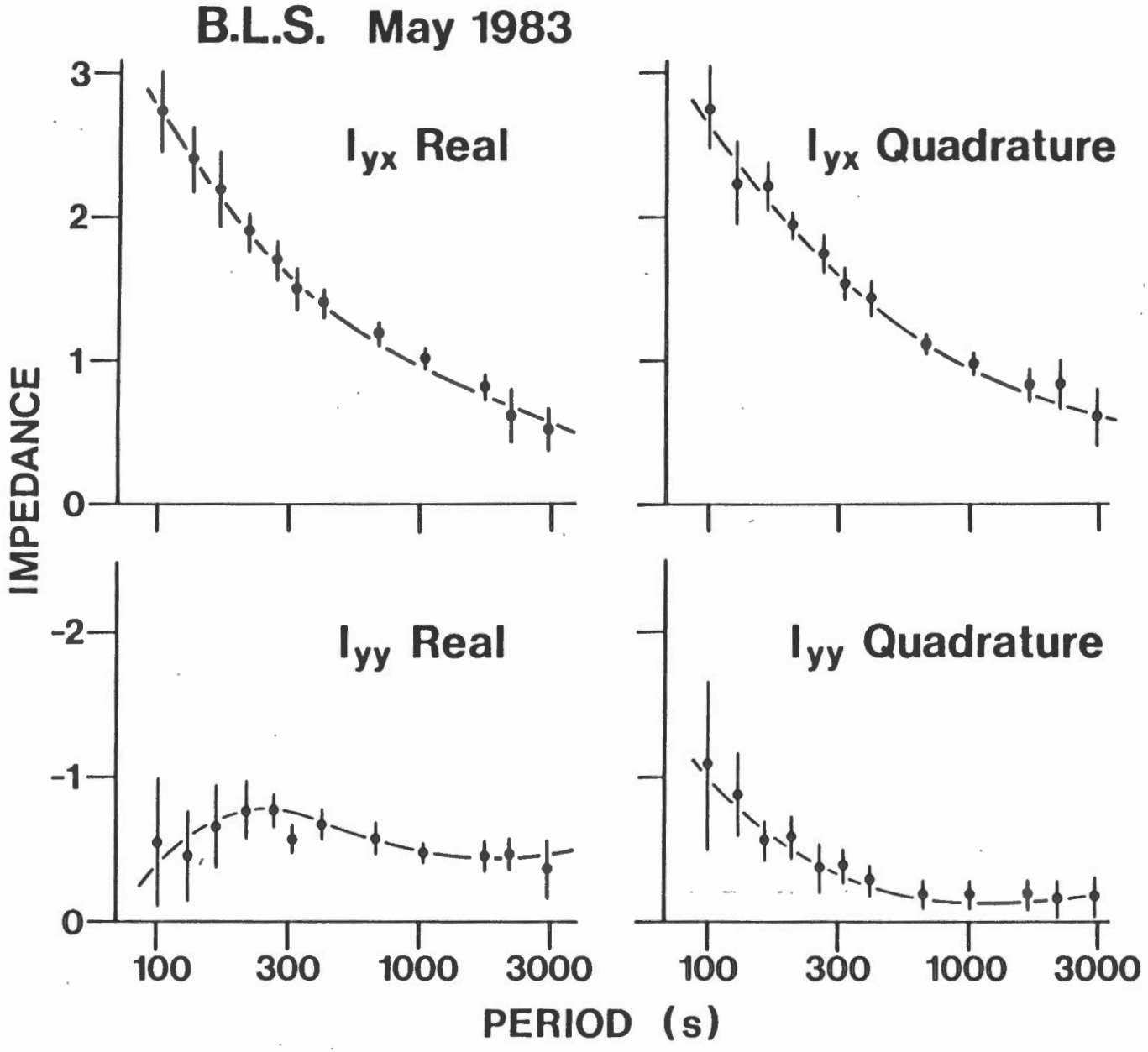

Fig. 9. I_{yx} and I_{yy} Impendance tensor elements, real and quadrature, derived from twenty second data from BLS

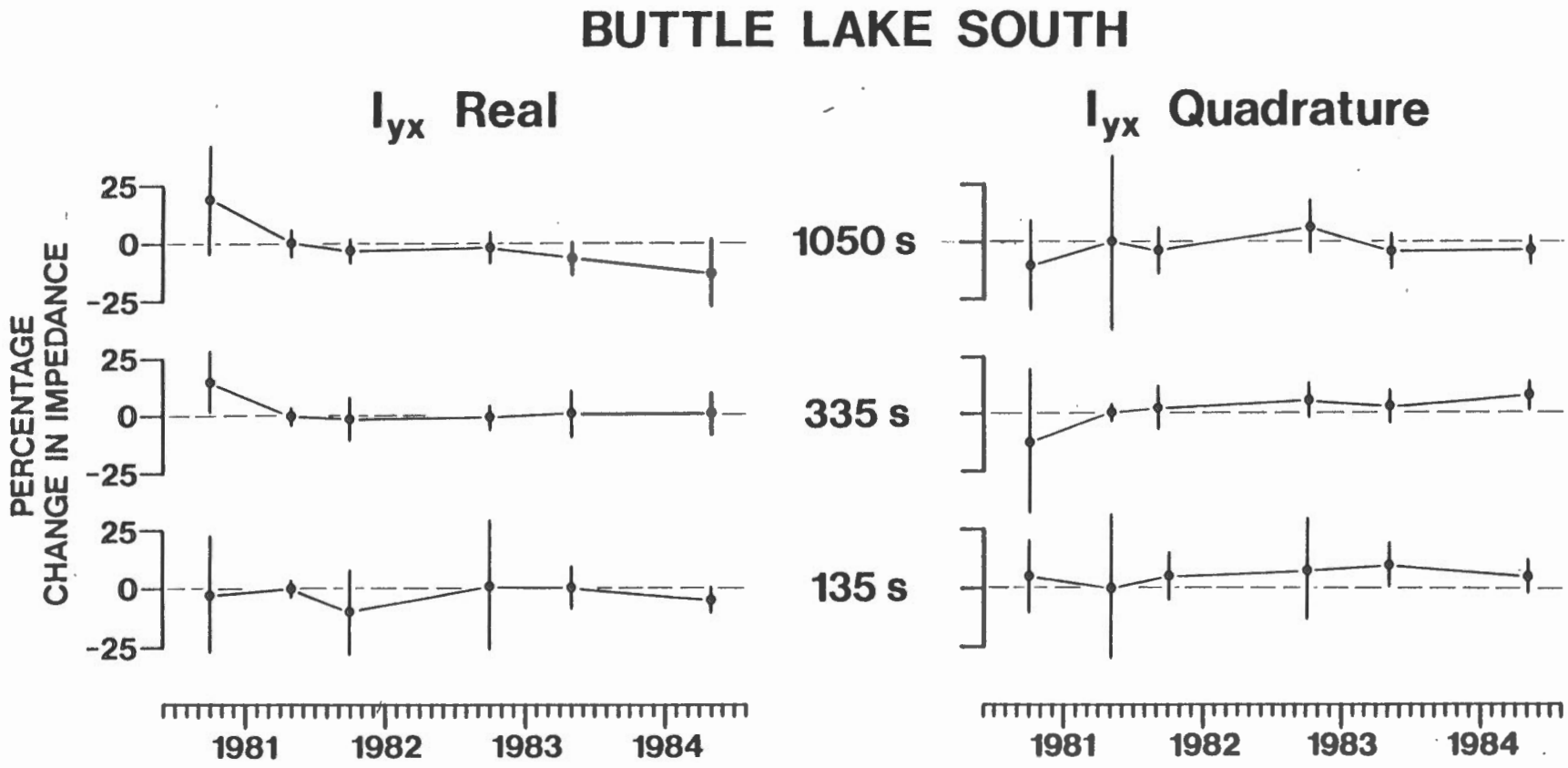

Fig. 10. Percentage change with time in the I_{yx}, Impendance tensor element, real and quadrature, at BLS

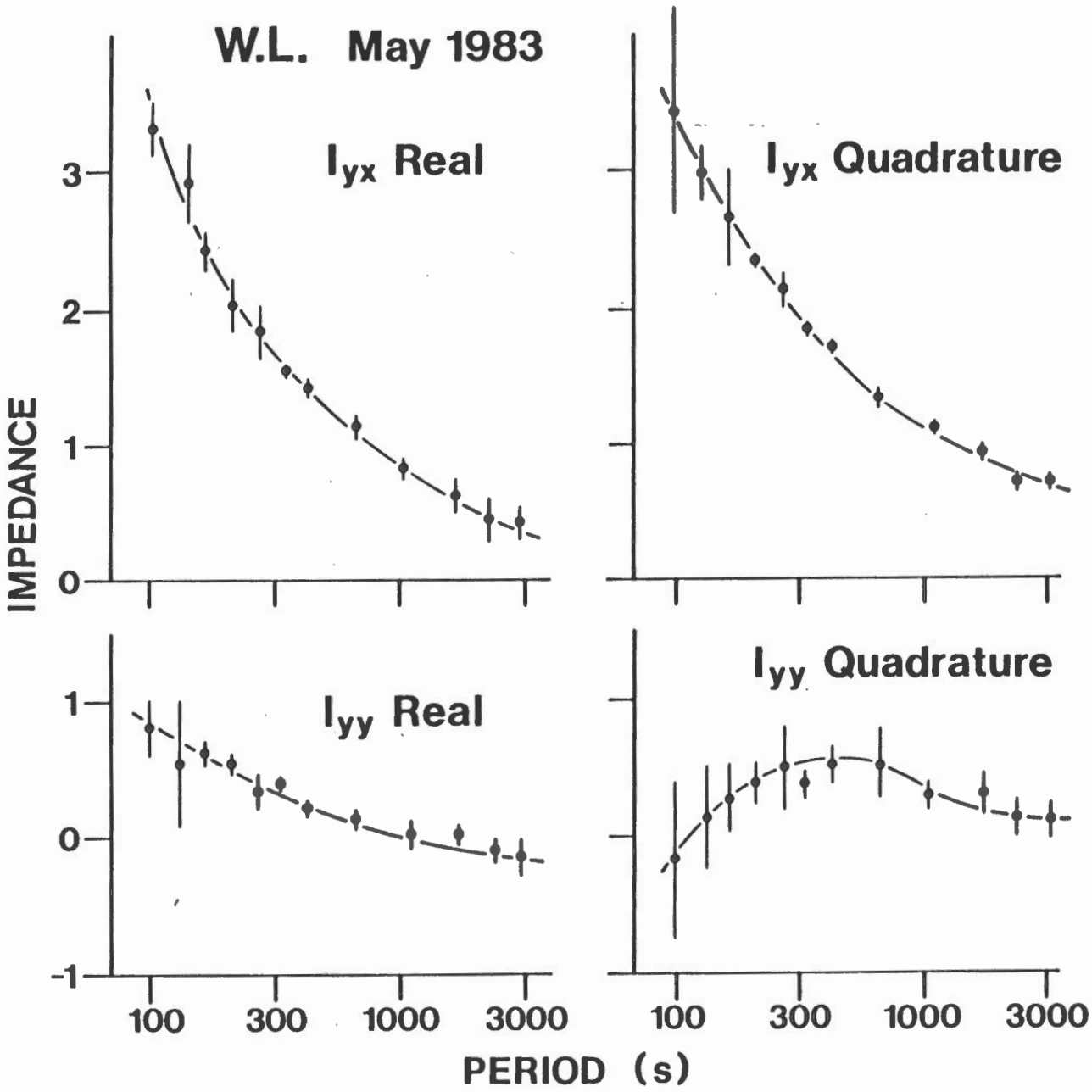

Fig. 11. I_{yx} and I_{yy} Impendance tensor elements, real and quadrature, derived from twenty second data from Wolf Lake

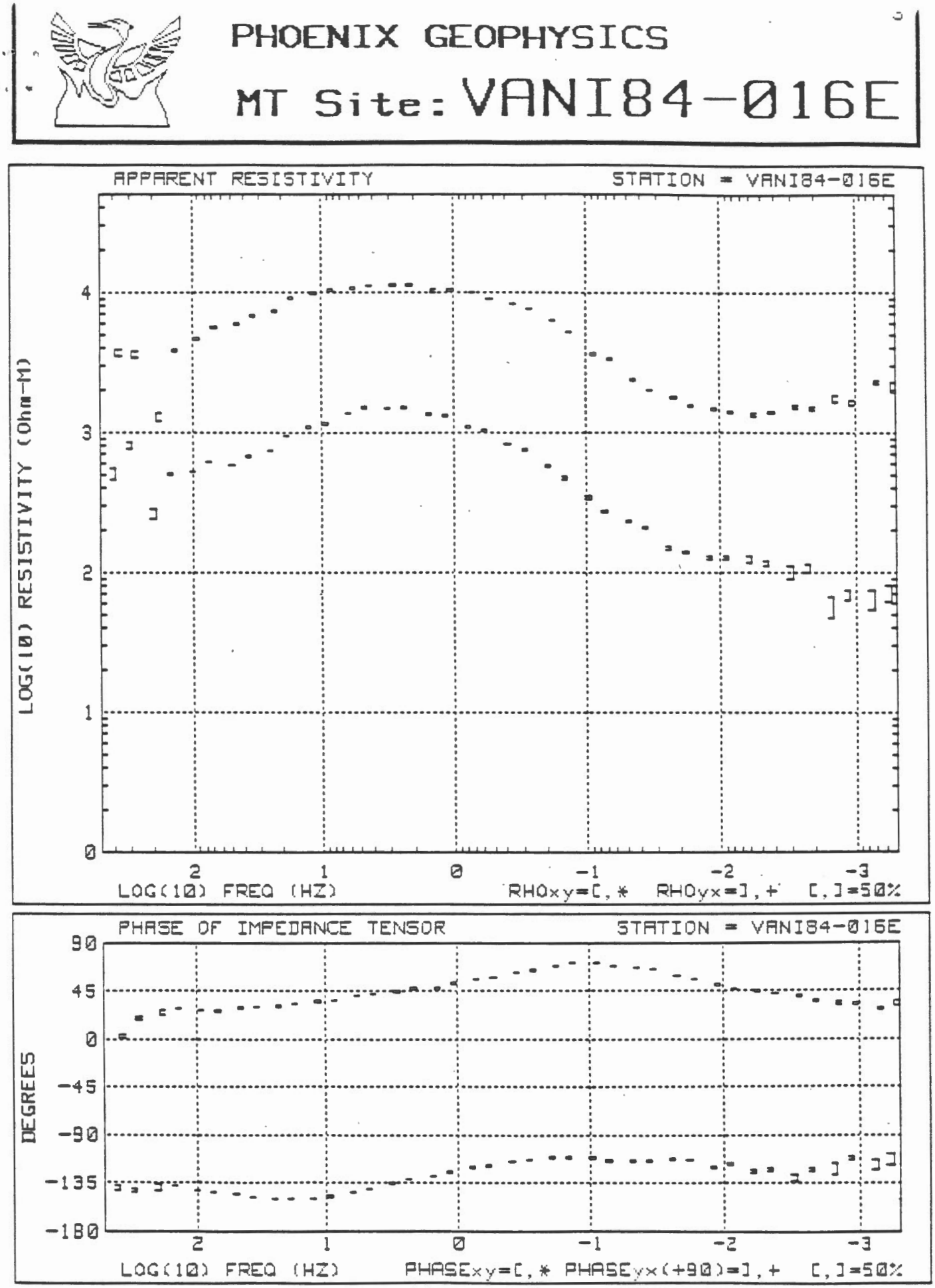

Fig. 12. Plot of apparent resistivity and phase versus period for the BLS site obtained directly from the output of the Phoenix Geophysics system